Applied Mathematics Letters 22 (2009) 1598–1603

Contents lists available at ScienceDirect

Applied Mathematics Letters

journal homepage: www.elsevier.com/locate/aml

Optimal die shape for film casting

K. Selvanayagam [a,b], T. Götz [b,*], S. Sundar [a], V. Vetrivel [a]

[a] Department of Mathematics, IIT Madras, Chennai 600 036, India

[b] Department of Mathematics, University of Kaiserslautern, P.O. Box 3049, 67653 Kaiserslautern, Germany

ARTICLE INFO

Article history:
Received 1 September 2008
Accepted 1 September 2008

Keywords:
Film casting process
Hyperbolic equation

ABSTRACT

We consider an isothermal model for the film casting process. The aim of this study is to determine a shape of the die that leads to a uniform thickness of the film. Thanks to a decoupling of the equations for the thickness and the velocities of the film, we are able to solve the reverse thickness equation. This reverse equation describes the dependence of the shape of the die on the desired final thickness.

1. Modelling film casting processes

Polymer films for video and magnetic tapes are produced by film casting. Molten polymer emerging from a flat die is stretched between the die and a temperature controlled roll. The film shows a lateral neck-in as well as an inhomogeneous decrease of the thickness. The final film is thicker at the edges than at the middle part; this effect is the so-called edge bead defect. In this work we determine a shape of the die that minimizes the edge bead defect.

For simplicity, we consider the stationary, isothermal three-dimensional Newtonian model for the film casting process derived earlier by Demay and co-workers [1–3] and in [4]. The geometry of the film casting process is shown in Fig. 1.1. The polymer is pressed through the die (located in the yz-plane) with a velocity u_0 and wrapped up with velocity $u_L > u_0$ by a spindle at $x = L$. The die has a width of W_0 in the y-direction and a thickness of e_0 in the z-direction. For typical film casting processes, the thickness of the film at the nozzle is small compared to both the length and the width of the film, i.e. $e_0/W_0 \ll 1$ and $e_0/L \ll 1$. We average the mass and momentum equations describing the polymer flow over the z-direction. This leads to the following reduced equations (see [1,2]):

$$\nabla \cdot (eU) = 0 \tag{1.1a}$$

$$(U \cdot \nabla)U = \frac{1}{\mathrm{Re}} \left(\Delta U + 3\nabla (\nabla \cdot U) \right). \tag{1.1b}$$

Here $U = (u, v)$ denotes the velocity field in the x- and y-directions and e denotes the thickness of the film in the z-direction. The Reynolds number $\mathrm{Re} = \frac{Lu_L}{\nu}$ is based on the length of the film, the take-up velocity and the viscosity of the fluid. Using the notation of Fig. 1.1, the system (1.1) has to be solved inside the two-dimensional film domain $\Omega = \{(x, y) : 0 < x < L, \ -W(x) < y < W(x)\}$. Note that the width $W(x)$ of the film is a free boundary and not known a priori. The boundary of the domain consists of the extrusion line $\gamma_1 = \{0\} \times (-W(0), W(0))$, the take-up line $\gamma_2 = \{L\} \times (-W(L), W(L))$ and the lateral boundaries $\gamma_3 = (0, L) \times \{-W(x)\}$ and $\gamma_4 = (0, L) \times \{W(x)\}$. At the inflow and outflow flow boundaries, we prescribe Dirichlet data

$$(u,\ v,\ e) = (u_0,\ 0,\ e_0) \quad \text{at } \gamma_1\ , \tag{1.1c}$$

$$(u,\ v) = (u_L,\ 0) \quad \text{at } \gamma_2. \tag{1.1d}$$

* Corresponding author.
E-mail address: goetz@mathematik.uni-kl.de (T. Götz).

0893-9659/$ – see front matter
doi:10.1016/j.aml.2008.09.007

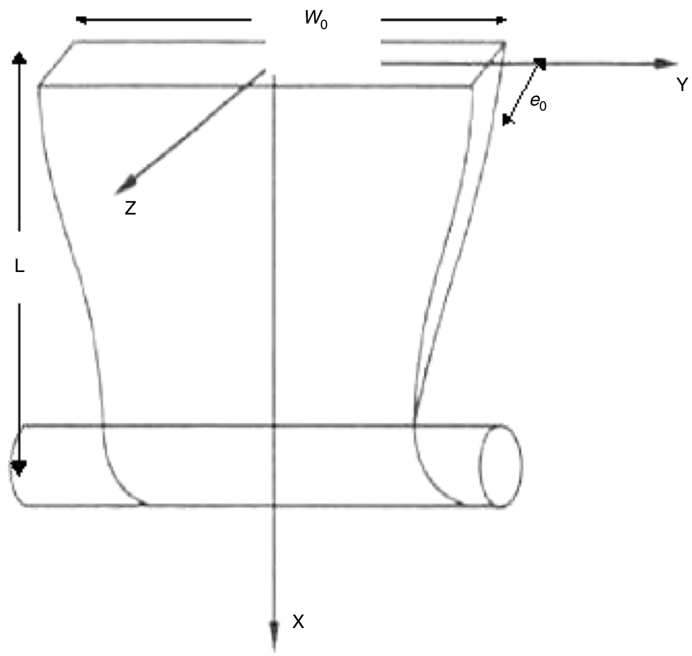

Fig. 1.1. Sketch of the geometry considered for the film casting process.

The ratio $D = u_L/u_0 > 1$ between the winding and the extrusion velocity is called the draw ratio. Due to the hyperbolic nature of Eq. (1.1a), there is no boundary condition for the thickness on γ_2. The treatment of the lateral boundaries γ_3, γ_4 is more sophisticated, since they are free boundaries. Their location is not known in advance and evolves with the width $W = W(x)$ of the film. The dynamic and kinematic conditions along the free boundary read as

$$\sigma \cdot n = 0 \quad \text{at } \gamma_3,\ \gamma_4\ , \tag{1.1e}$$

$$u\partial_x W - v = 0 \quad \text{at } \gamma_3, \gamma_4. \tag{1.1f}$$

Here n denotes the unit outer normal to γ_i, $i = 3, 4$. The stress tensor σ is given by $\sigma = (\nabla U) + (\nabla U)^{\mathrm{T}} + 2\,(\operatorname{div} U)\, I = \begin{pmatrix} 4\partial_x u + 2\partial_y v & \partial_y u + \partial_x v \\ \partial_y u + \partial_x v & 2\partial_x u + 4\partial_y v \end{pmatrix}$, where I is the 2×2 identity matrix.

The following typical parameters are used throughout the work: stretching distance $L = 0.4$ m, film width $W_0 = 1$ m, draw ratio $D = 10$ and Reynolds number Re $= 3$.

The model (1.1) is capable of predicting the final thickness $e(L, y)$ of the film. This thickness profile depends on the geometry e_0 of the nozzle as well as the draw ratio D. Using a rectangular nozzle, i.e. a uniform initial thickness e_0, one obtains the well-known effect of edge beads; see Fig. 1.2. In this case the final film is thinner in the middle than at the lateral surfaces; an undesired result. In contrast to that, industrial applications aim to produce films with a uniform thickness profile at the take-up roll.

2. Optimal shape of the die

In the system (1.1), the velocity components u and v and the film width W are independent of the thickness e. Hence, we may compute the velocities in advance and solve the hyperbolic thickness equation (1.1a) afterwards. Note, that the flow is oriented in the positive x-direction; see Fig. 1.3.

For solving the thickness equation (1.1a) we only need one boundary condition at $x = 0$, i.e. at the nozzle. For a constant thickness at the nozzle we obtain the undesired edge bead defect. To overcome this edge bead defect, we consider the thickness equation with a reverse flow direction (Fig. 1.4)

$$\partial_x(-eu) + \partial_y(-ev) = 0 \qquad \text{and} \qquad e = e_d \quad \text{at } \gamma_2. \tag{2.1}$$

For this reverse thickness equation, we prescribe the desired thickness at the chill roll e_d and solve backwards to obtain the thickness at the die $e(0, y)$. This thickness at the die equals the desired shape of the die leading to the constant film thickness at the take-up roll.

3. Numerical solution

Since the boundaries γ_3 and γ_4 are free surfaces, it is difficult to implement the boundary condition $\sigma \cdot n = 0$. Hence, we apply the transformation $\Phi : \Omega \to [0, L] \times [-1, 1]$, $\Phi(x, y) = (x, \tilde{y})$, where $\tilde{y}(x) = \frac{y}{W(x)}$, to the system (1.1). Now, the

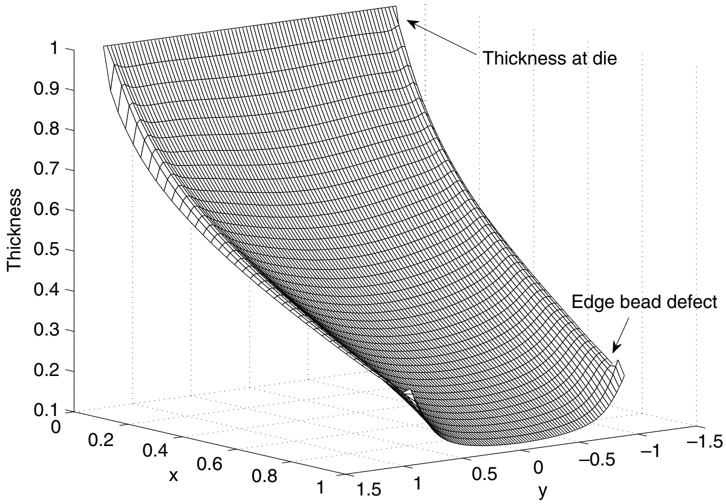

Fig. 1.2. Thickness profile of the film casting process with edge bead defect.

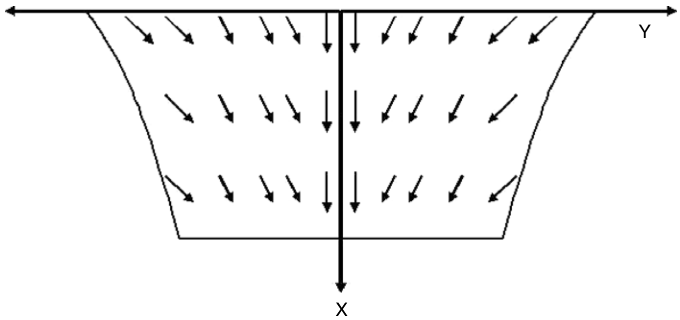

Fig. 1.3. Flow direction in the original problem (1.1a).

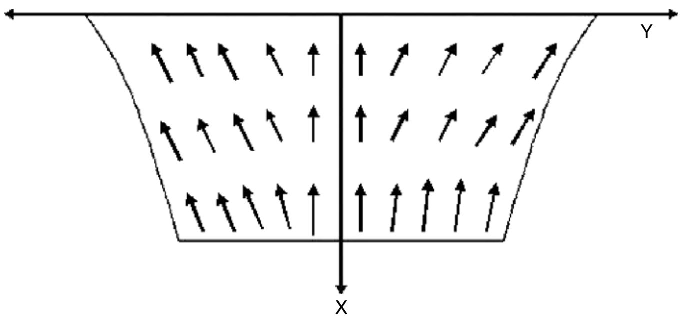

Fig. 1.4. Flow direction in the reverse problem (2.1).

momentum equations (1.1b) together with the transformed dynamic boundary condition (1.1e) can be solved on the fixed domain $[0, L] \times [-1, 1]$ for the velocities u and v. Afterwards, we determine the film width W from the kinematic condition (1.1f), i.e. $W' = v/u$ and $W(0) = W_0$. These steps are iterated until convergence is reached. In the final step, the film thickness is computed using (2.1).

To discretize the PDEs, we use finite differences on a uniform grid with mesh widths $h, \ k > 0$ in the x- and $\tilde{y}$-directions. Central differences are used in the momentum equation (1.1b), and the nonlinear terms are handled by iteration. For the reverse mass equation (2.1) an upwind method is applied. Since the transport in Eq. (2.1) is oriented in the negative

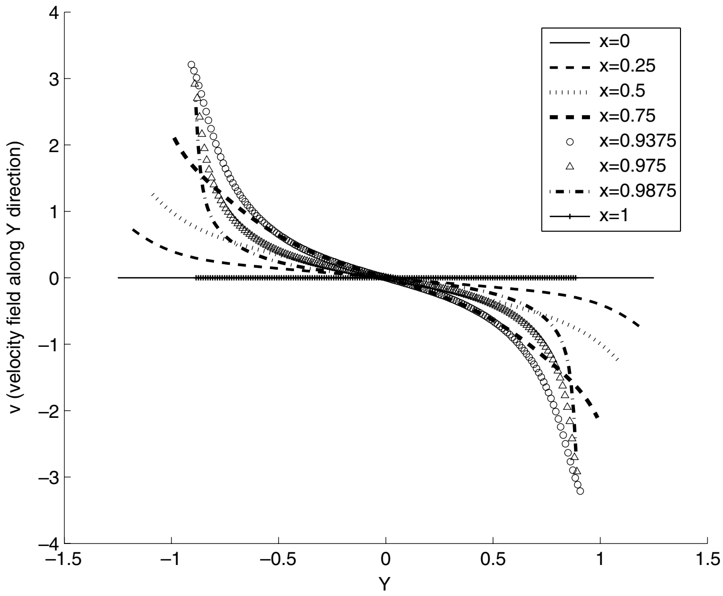

Fig. 4.1. Transverse velocity v.

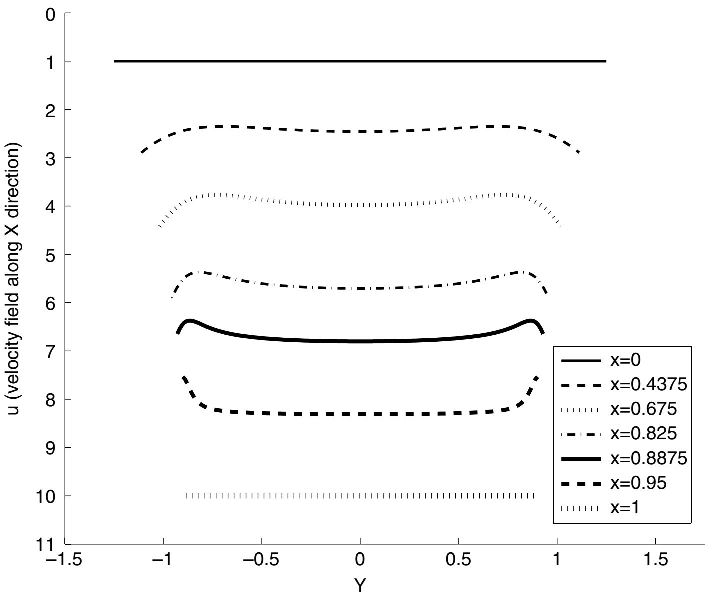

Fig. 4.2. Longitudinal velocity u.

x-direction, the upwind scheme reads as

$$\frac{(eu)_{i+1j}-(eu)_{ij}}{h}-y\frac{W'}{W}\frac{(eu)_{ij+1}-(eu)_{ij-1}}{2k}+\frac{1}{W}\frac{(ev)_{ij}-(ev)_{ij-1}}{k}=0,$$

where u_{ij} denotes the value of u at the grid point $(x_i,\tilde{y}_j)=(ih,jk)$.

4. Simulation results

In the first step, we solved the system (1.1) for a given constant initial thickness e_0. Fig. 1.2 shows the thickness of the film. The transverse velocity component v at different lateral cuts $x=x_i$ is shown in Fig. 4.1. The velocities are negative in the region $y>0$ and positive in the region $y<0$. This implies that the fluid moves towards the centerline $y=0$ and hence we obtain the neck-in of the film.

Fig. 4.2 shows the longitudinal velocity component $u(\cdot,y)$ at different lateral cuts, analogous to Fig. 4.1. The increase of the longitudinal velocity due to the draw ratio $D>1$ is clearly visible.

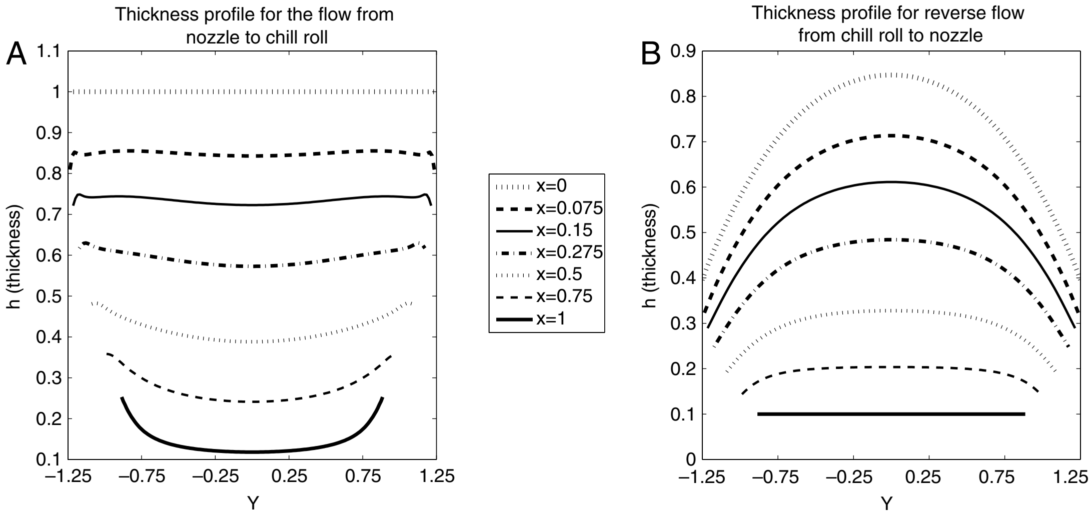

Fig. 4.3. Film thickness e in original problem (A) and film thickness e in reverse problem (B).

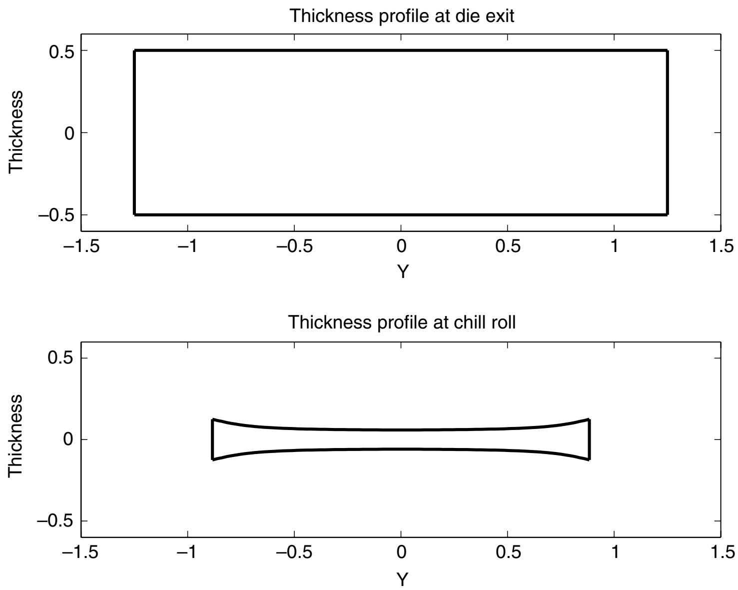

Fig. 4.4. Original nozzle shape (top) and computed film thickness at take-up (bottom).

Fig. 4.3(A) and 4.3(B) show the film thickness $e(\cdot, y)$ at different lateral cuts x_i for the original (A) and the reverse problem (B), respectively. Fig. 4.3(A) shows the development of the edge bead for a rectangular shape of the die. On the other hand, from Fig. 4.3(B) we can determine the shape of the die that leads to a constant thickness at the chill roll.

Fig. 4.4 shows the original, uniform shape of the die (top) and the resulting film thickness (bottom). The edge bead defect is clearly visible. Fig. 4.5 shows the computed, uniform thickness of the film (bottom). The barrel shape of the nozzle compensated the neck-in of the film and hence yields the desired uniform thickness.

5. Conclusion

We studied the isothermal film casting process. On the basis of the averaged Navier–Stokes equations, the evolution of the film thickness and width is governed by a free boundary value problem. The uniform thickness profile at the nozzle always leads to the so-called edge bead effect; the final film gets thinner in the middle than at the edges. Hence we consider a reverse flow to determine the optimal shape of the nozzle that will lead to an even thickness distribution at the take-up point.

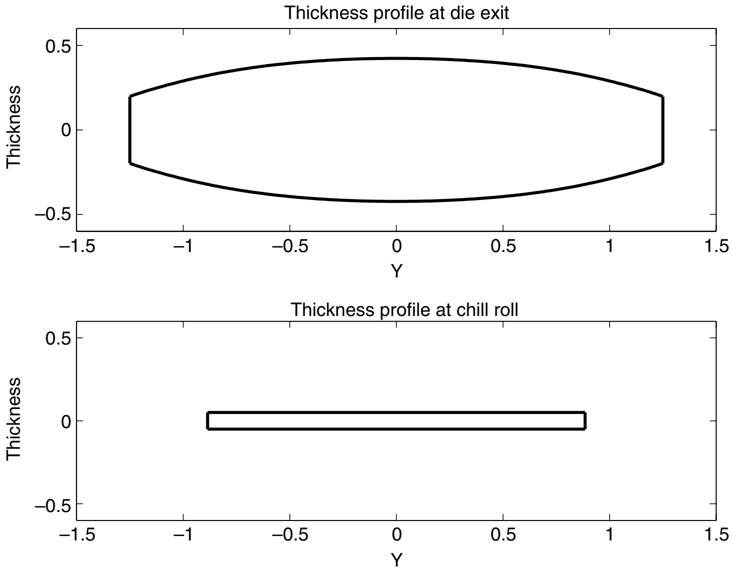

Fig. 4.5. Computed nozzle shape (top) and film thickness at take-up (bottom).

References

[1] S. d'Halewyu, J.F. Agassant, Y. Demay, Numerical simulation of the cast film process, Polym. Eng. Sci. 30 (1990) 335–340.
[2] D. Silagy, Y. Demay, J.F. Agassant, Numerical simulation of the film casting process, Int. J. Numer. Methods Fluids 30 (1999) 1–18.
[3] A. Fortin, P. Carrier, Y. Demay, Numerical simulation of coextrusion and film casting, Int. J. Numer. Methods Fluids 20 (1995) 31–57.
[4] P. Barq, J.M. Haudin, J.F. Agassant, Isothermal and anisothermal models for cast film extrusion, Intern. Polym. Process. VII (4) (1992) 334–349.